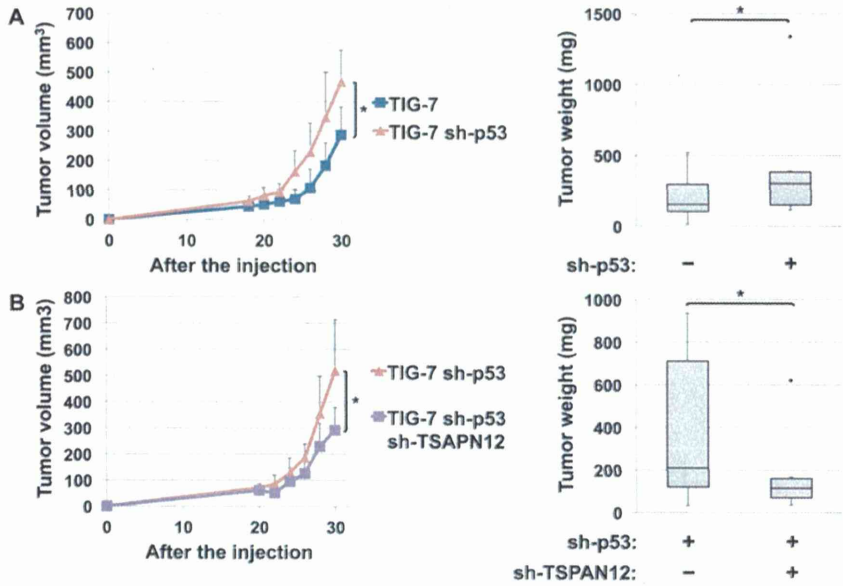

Fig. S7. TSPAN12 regulated tumor growth enhanced by p53-depleted fibroblasts. (*A*) Four weeks after the inoculation, the tumor volume (*Left*) and tumor weight (*Right*) of the H1299-LUC xenograft tumor mixed with either parental TIG-7 cells or p53-depleted TIG-7 cells were measured ($n = 4$ per group, paired *t* test for tumor volume $^*P < 0.05$; $n = 8$ per group, Wilcoxon signed-rank test for tumor weight $^*P < 0.05$). (*Left* back) Coinjection with parental TIG-7 cells. (*Right* back) Coinjection with p53-depleted TIG-7 cells. (*B*) Four weeks after the inoculation, the tumor volume (*Left*) and tumor weight (*Right*) of the H1299-LUC xenograft tumor mixed with either p53-depleted TIG-7 cells or p53-depleted TIG-7 cells expressing sh-TSPAN12 were measured ($n = 5$ per group, paired *t* test for tumor volume $^*P < 0.05$; $n = 9$ per group, Wilcoxon signed-rank test for tumor weight $^*P < 0.05$).

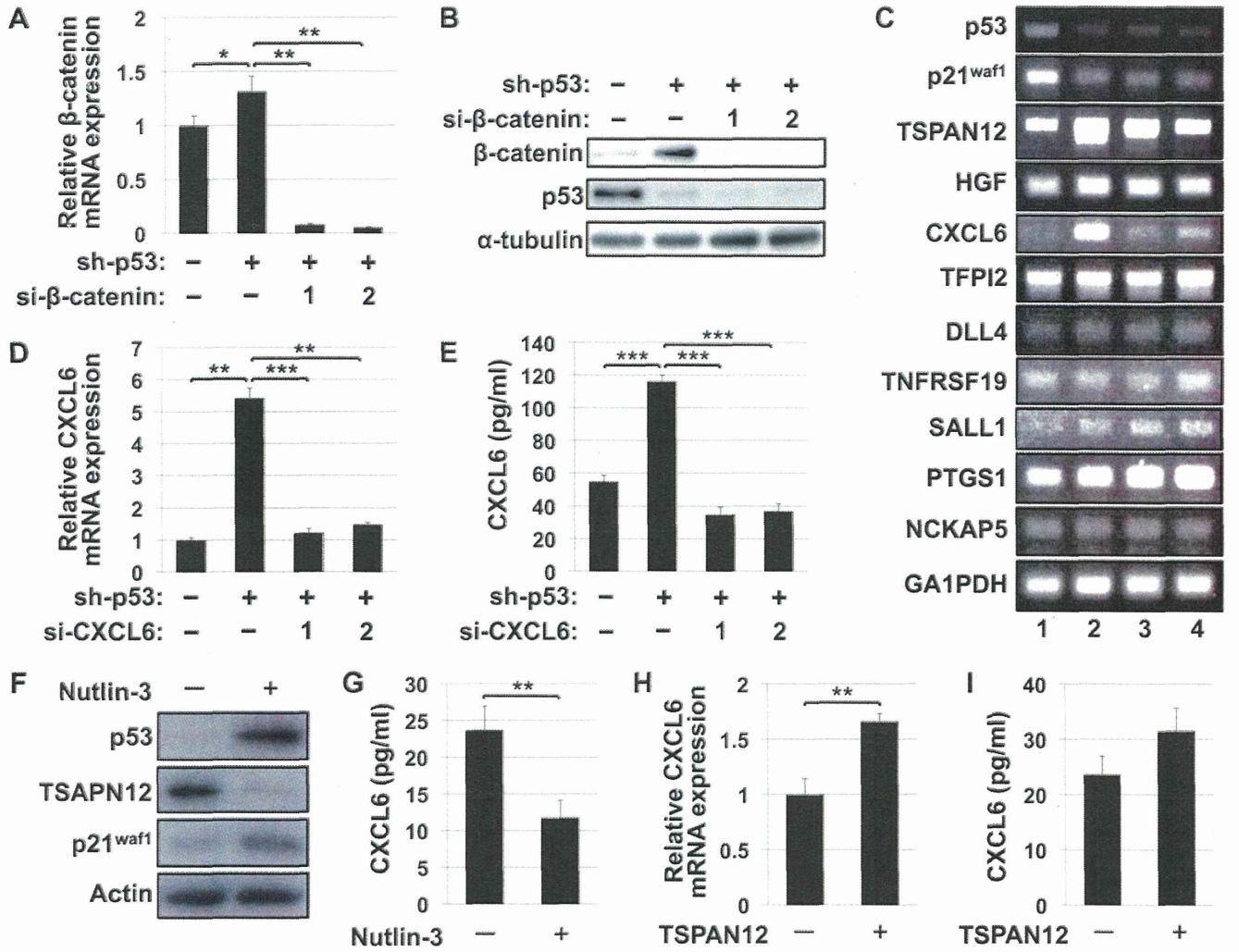

Fig. S8. (*A* and *B*) Decrease in β-catenin in TIG-7 cells by siRNAs. p53-depleted TIG-7 cells were transfected with control siRNAs or si–β-catenin. Expression levels of the indicated genes were determined by qRT-PCR (*A*) and immunoblotting (*B*). (*C*) Identification of CXCL6 as a p53-up-regulated TSPAN12-regulated gene. Expression levels of selected genes, which have the potential to function in cancer progression, including cell proliferation, invasion, and metastasis, were indicated using RNAs from TIG-7 cells by semiquantitative RT-PCR. Lane 1, parental TIG-7 cells; lane 2, p53-depleted TIG-7 cells transfected with control siRNAs; lane 3, p53-depleted TIG-7 cells transfected with si-TSPAN12#1; lane 4, p53-depleted TIG-7 cells transfected with si-TSPAN12#2. (*D* and *E*) Knockdown efficiency of CXCL6 in p53-depleted TIG-7 cells. p53-depleted TIG-7 cells were transfected with control siRNAs or si-CXCL6. The expression level of CXCL6 in cells depleted of CXCL6 was determined by qRT-PCR (*D*). The production of CXCL6 secreted from cells depleted of CXCL6 was quantified by ELISA (*E*). (*F* and *G*) TSPAN12 and CXCL6 were down-regulated by the treatment with nutlin-3. TIG-7 cells were treated with 10 μM of nutlin-3 for 24 h and the expression of the indicated proteins was determined by immunoblotting (*F*) and ELISA (*G*). (*H* and *I*) The overexpression of TSPAN12 in TIG-7 cells induced a slight increase in CXCL6. Expression levels of CXCL6 in parental or TSPAN12-expressed TIG-7 cells were determined by qRT-PCR (*H*) and ELISA (*I*). Data are the mean ± SD of three or more independent experiments. Statistical analyses were performed using the Student *t* test. $^{*}P < 0.05$, $^{**}P < 0.01$, $^{***}P < 0.001$.

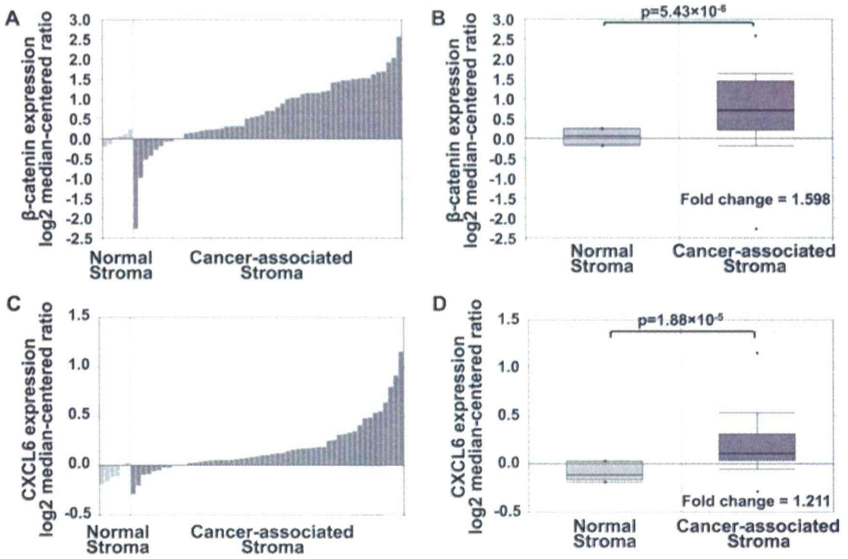

Fig. S9. Expression levels of β-catenin and CXCL6 were higher in breast cancer-associated stromal tissues than in normal stromal tissues. (*A* and *B*) Expression levels of β-catenin in 6 samples of normal stromal tissues and 53 samples of cancer-associated stromal tissues extracted from the Oncomine dataset are shown individually (*A*) and collectively (*B*). (*C* and *D*) Expression levels of CXCL6 in 6 samples of normal stromal tissues and 53 samples of cancer-associated stromal tissues extracted from the Oncomine dataset are shown individually (*C*) and collectively (*D*).

Table S1. p53-up-regulated genes encoding membrane proteins in fibroblasts

Representative public ID	Gene symbol	Gene title	Fold change
NM_001657	AREG / AREGB	Amphiregulin / amphiregulin B	24.217
NM_007287/AI433463	MME	Membrane metallo-endopeptidase	9.721/4.613*
NM_018057	SLC6A15	Solute carrier family 6 (neutral amino acid transporter), member 15	7.620
AA502609	TRPA1	Transient receptor potential cation channel, subfamily A, member 1	5.209
AB036931	DLL4	Delta-like 4 (*Drosophila*)	5.161
BF059512	DNER	Delta/notch-like EGF repeat containing	5.160
H20055	GRIA4	Glutamate receptor, ionotropic, AMPA 4	4.596
NM_012338	TSPAN12	Tetraspanin 12	4.580
NM_000640	IL13RA2	Interleukin 13 receptor, alpha 2	4.551
X68742	ITGA1	Integrin, alpha 1	3.968
AI680986/R70320	SLITRK6	SLIT and NTRK-like family, member 6	3.618/3.541*
AI873273	SLC16A6	Solute carrier family 16, member 6 (monocarboxylic acid transporter 7)	3.612
NM_001993	F3	Coagulation factor III (thromboplastin, tissue factor)	3.355
AW274018	LPAR3	Lysophosphatidic acid receptor 3	3.233
BF432648	TNFRSF19	Tumor necrosis factor receptor superfamily, member 19	3.000

*Threefold changes were detected because this gene was located at two distinct probes on the microarray.

Cell Reports
Article

TSPAN2 Is Involved in Cell Invasion and Motility during Lung Cancer Progression

Chihiro Otsubo,[1,2,9] Ryo Otomo,[1,2] Makoto Miyazaki,[1,2] Yuko Matsushima-Hibiya,[1] Takashi Kohno,[3] Reika Iwakawa,[3] Fumitaka Takeshita,[4] Hirokazu Okayama,[3,10] Hitoshi Ichikawa,[5] Hideyuki Saya,[6] Tohru Kiyono,[7] Takahiro Ochiya,[4] Fumio Tashiro,[2] Hitoshi Nakagama,[8] Jun Yokota,[3] and Masato Enari[1,*]

[1]Division of Refractory Cancer Research, National Cancer Center Research Institute, Chuo-ku, Tokyo 104-0045, Japan
[2]Department of Biological Science and Technology, Faculty of Industrial Science and Technology, Tokyo University of Science, Katsushika-ku, Tokyo 125-8585, Japan
[3]Division of Genome Biology, National Cancer Center Research Institute, Chuo-ku, Tokyo 104-0045, Japan
[4]Division of Molecular and Cellular Medicine, National Cancer Center Research Institute, Chuo-ku, Tokyo 104-0045, Japan
[5]Division of Genetics, National Cancer Center Research Institute, Chuo-ku, Tokyo 104-0045, Japan
[6]Division of Gene Regulation, Institute for Advanced Medical Research, School of Medicine, Keio University, Shinjuku-ku, Tokyo 160-8582, Japan
[7]Division of Virology, National Cancer Center Research Institute, Chuo-ku, Tokyo 104-0045, Japan
[8]Division of Cancer Development System, National Cancer Center Research Institute, Chuo-ku, Tokyo 104-0045, Japan
[9]Present address: Kobe University Graduate School of Medicine, Chuo-ku, Kobe, Hyogo 650-0017, Japan
[10]Present address: Laboratory of Human Carcinogenesis, Center for Cancer Research, National Cancer Institute, National Institutes of Health, Bethesda, MD 20892, USA
*Correspondence: menari@ncc.go.jp
http://dx.doi.org/10.1016/j.celrep.2014.03.027

SUMMARY

In lung cancer progression, p53 mutations are more often observed in invasive tumors than in noninvasive tumors, suggesting that p53 is involved in tumor invasion and metastasis. To understand the nature of p53 function as a tumor suppressor, it is crucial to elucidate the detailed mechanism of the alteration in epithelial cells that follow oncogenic KRAS activation and p53 inactivation. Here, we report that KRAS activation induces epithelial-mesenchymal transition and that p53 inactivation is required for cell motility and invasiveness. Furthermore, TSPAN2, a transmembrane protein, is responsible for cell motility and invasiveness elicited by p53 inactivation. TSPAN2 is highly expressed in p53-mutated lung cancer cells, and high expression of TSPAN2 is associated with the poor prognosis of lung adenocarinomas. TSPAN2 knockdown suppresses metastasis to the lungs and liver, enabling prolonged survival. TSPAN2 enhances cell motility and invasiveness by assisting CD44 in scavenging intracellular reactive oxygen species.

INTRODUCTION

The tumor suppressor protein p53 responds to various stimuli, including genotoxic stresses and oncogenic activation, and activates the transcription of numerous target genes involved in cell-cycle arrest and apoptosis to prevent tumor cell growth (Bourdon et al., 2003; Lane and Levine, 2010; Oren, 2003). Thus, one of the functions of p53 is to induce irreversible cell growth (Zuckerman et al., 2009). On the other hand, clinicopathological studies of lung specimens have implied that p53 is also involved in tumor invasion and metastasis because p53 inactivation is more often observed in invasive tumors than in noninvasive tumors in lung cancer progression (Iwakawa et al., 2008; Robles and Harris, 2010). Indeed, several lines of recent evidence have shown that p53 regulates invasion and cell motility, which are associated with aggressive and metastatic phenotypes of cancer cells (Aylon and Oren, 2011; Gadea et al., 2007; Muller et al., 2011; Vinot et al., 2008).

Lung adenocarcinomas (ADCs) have been thought to arise from the accumulation of various genetic alterations, including oncogenic activation, such as KRAS and epidermal growth factor receptor (EGF-R) and tumor suppressor inactivation, such as p16INK4A and p53 in small airway epithelial cells (SAECs), which are the putative origin of lung ADCs (Forgacs et al., 2001; Majidi et al., 2007; Sato et al., 2006). In particular, the p53 pathway is inactivated in most lung ADCs and is a key regulator of invasive phenotypic transition (Iwakawa et al., 2008). Epithelial-mesenchymal transition (EMT) is regarded as an important event for triggering invasion and dissemination from primary tumors (Biddle and Mackenzie, 2012). Snail and Twist are known as EMT inducers and p53 inactivation promotes EMT by derepressing Snail expression and upregulating Twist expression (Kim et al., 2011; Kogan-Sakin et al., 2011).

Although there are many factors contributing to lung cancer progression, including invasiveness and metastasis, the detailed molecular mechanism of how p53 contributes to lung cancer progression is unknown. In particular, gene regulation depends on cellular contents, and it is crucial to identify p53-related

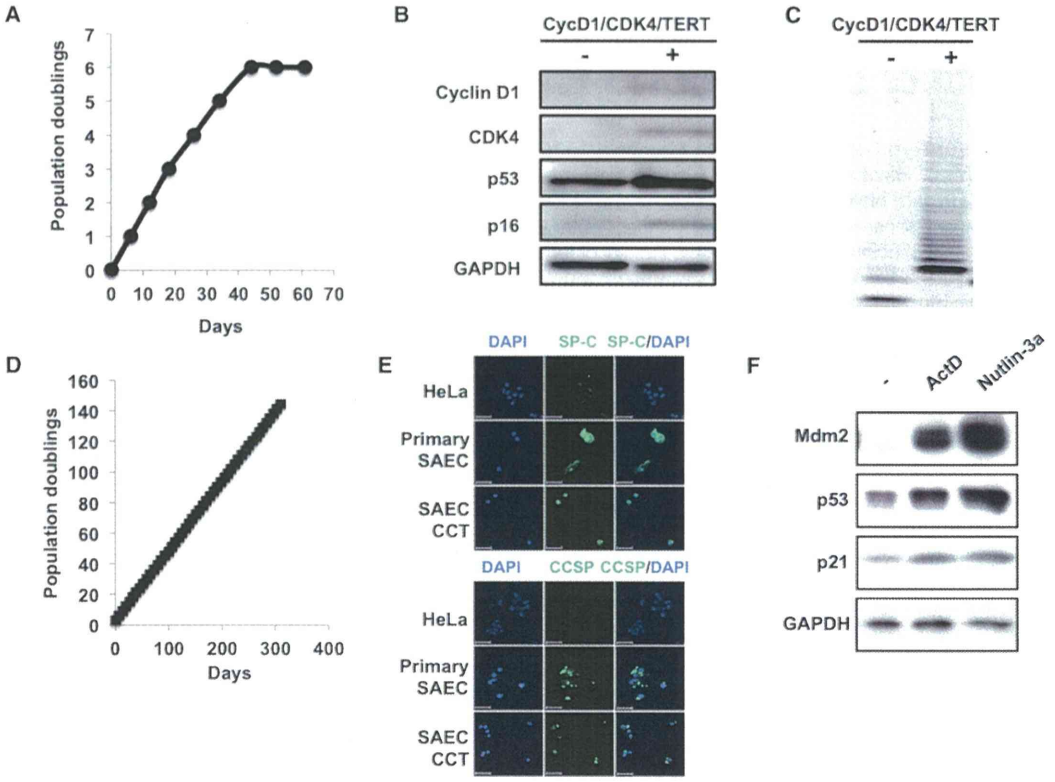

Figure 1. Immortalized SAECs Are Intact in the p53 Pathway

(A) Cell growth curve of parental SAECs is shown. Cells were grown in SAGM and maintained by passaging at 1–2 dilution and changing medium every 3 days.

(B) Expression levels of transduced proteins in parental SAECs are shown by immunoblot analysis. GAPDH is shown as a loading control.

(C) Telomerase activity is detectable in SAECs infected with CycD1, CDK4, and TERT lentiviruses but not parental SAECs.

(D) Cell growth curve of immortalized SAECs is shown. Cells were grown in SAGM and maintained by passaging at 1–8 dilution.

(E) Immortalized SAECs are exhibited lung epithelial features. Expression of lung epithelial markers, SP-C and CCSP, in primary and immortalized SAECs (SAEC CCT) but not HeLa cells (negative control) was detected by immunofluorescence.

(F) p53 is activated in immortalized SAECs in response to actinomycin D (ActD) and Nutlin-3a. Cells were incubated in the absence or presence of 5 nM ActD or 10 μM Nutlin-3a for 16 hr, and these cell lysates were subjected to immunoblotting. GAPDH is shown as a loading control.

factors using an appropriate cell system. In this study, we established a system to elucidate the detailed mechanism of the alteration of epithelial cells, the main origin of solid tumors, such as lung cancers, following KRAS activation and p53 inactivation. Using this system, we found that KRAS activation was linked to EMT and that p53 inactivation enhanced cell motility and invasiveness. Furthermore, we identified a key molecule derepressed by p53 inactivation, as a factor responsible for the promotion of cell motility and invasiveness in lung ADCs. Intriguingly, p53 knockdown increases invasiveness and cell motility in various lung cancer cells through the derepression of TSPAN2 belonging to a family of four transmembrane-spanning protein. TSPAN2 expression was associated with the p53 mutation status and poor prognosis in lung ADCs, and the suppression of TSPAN2 expression inhibited cell motility and invasion, consequently preventing metastasis to the lungs. Finally, we elucidated that TSPAN2 scavenged intracellular reactive oxygen species through the CD44-mediated pathway to enhance cell motility and invasiveness.

RESULTS

KRAS Activation Induces EMT, and p53 Inactivation Enhances Cell Invasion and Motility in SAECs

SAECs were able to grow in conditioned medium for a while, but cells stopped growing and exhibited a senescent phenotype through the upregulation of p16INK4A, a cell-cycle inhibitor, after five to six population doublings (PDs) (Figures 1A and 1B). Slight increases of p53 and p16INK4A may be due to oxidative stress during cell culture (Rayess et al., 2012). Therefore, primary SAECs were immortalized by the expression of a mutant form of CDK4 devoid of binding ability to p16INK4A, CyclinD1, and TERT to bypass p16INK4A-mediated senescence and prevent telomere erosion. Immunoblotting analyses showed the expressions of CDK4, CyclinD1, and p16INK4A in SAECs (Figure 1B). We also confirmed TERT activity in immortalized cell lines using the telomeric repeat amplification protocol (TRAP) assay (Figure 1C), and immortalization of SAECs was successful, because cells continued to grow even after 144 PDs (Figure 1D). Next, we

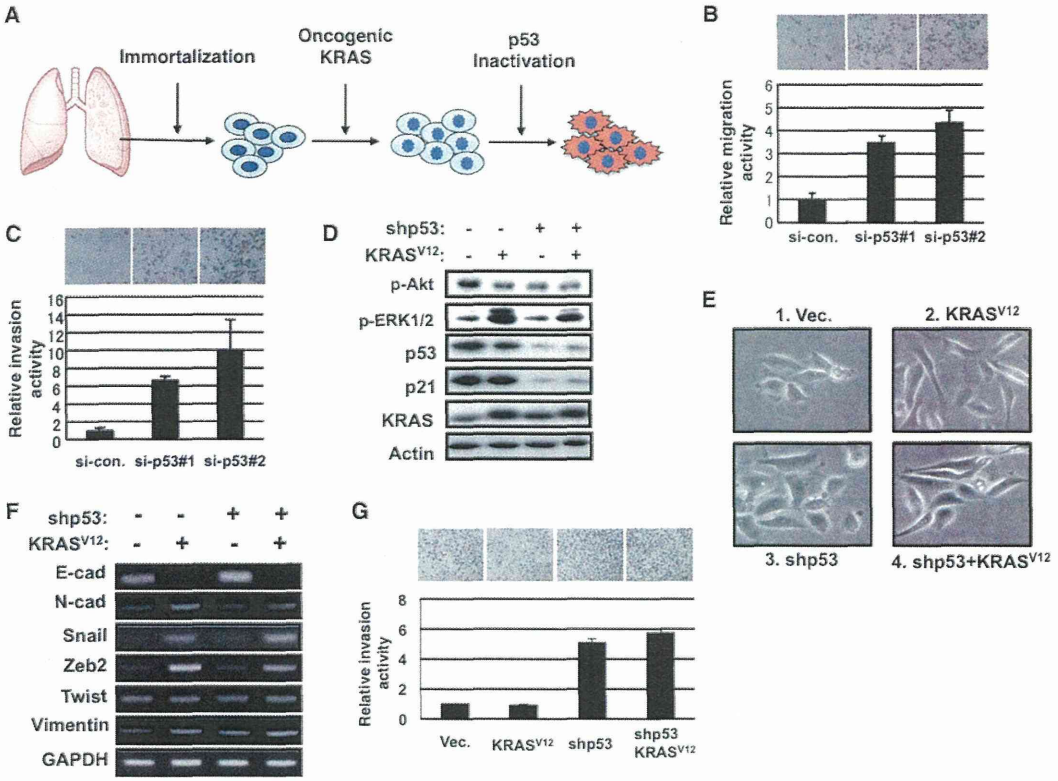

Figure 2. p53 Inactivation, but Not KRAS, which Induces an Epithelial-Mesenchymal Transition-like Phenotype, Enhances Cell Invasion and Motility in Immortalized Small Airway Epithelial Cells

(A) A mimetic system with genetic alternations in human epithelial cells during lung carcinogenesis is represented.

(B and C) p53 knockdown is enhanced motility (B) and invasiveness (C) in immortalized SAECs. Cells were transfected with the indicated siRNAs, and in vitro cell migration and invasion assays using cell-culture inserts were performed, as described in Experimental Procedures. Relative activities to the control siRNA are shown.

(D) Expression levels in immortalized SAECs infected with indicated viruses are shown. Cells were infected with either control viruses or $KRAS^{V12}$ expression viruses, followed by infection with either control viruses or p53-directed short-hairpin double-stranded RNAs (shp53) expression viruses. Expression levels of indicated proteins in these cell lysates were determined by immunoblotting.

(E) Morphological change of immortalized SAECs by expression of $KRAS^{V12}$ but not p53 knockdown. Stable transformants in (D) were observed under a differential interference contrast microscope.

(F) Induction of EMT-like property by $KRAS^{V12}$ expression but not p53 knockdown. Expression levels of EMT-related genes altered by $KRAS^{V12}$ expression were determined by RT-PCR.

(G) $KRAS^{V12}$ expression did not influence invasive activity in immortalized SAECs. Invaded cells were stained with Diff-Quick solution, and stained cells were counted under a light microscope. Relative activities to the control cells are shown.

Error bars indicate SD of three independent measurements.

confirmed that these cells maintained the characteristics of primary SAECs as assayed by immunofluorescence for surfactant protein C (SP-C) and Clara cell secretory protein (CCSP), which are differentiation and functional markers for alveolar epithelial type II cells (AEC2) and Clara cells, respectively (Lundin and Driscoll, 2013). As shown in Figure 1E, SAECs, but not HeLa (negative control), were expressed SP-C and CCSP, suggesting that they exhibit typical characteristics of human lung epithelial cells and are likely to be a heterogeneous population containing AEC2, Clara cells, and bronchioalveolar stem cells (BASCs) (Lundin and Driscoll, 2013). To test whether the p53 pathway is still intact, immortalized cells were treated with DNA-damaging agents. Accumulation of p53 was detected, and $p21^{waf1}$ and Mdm2, p53 target genes, were upregulated in response to DNA damage, such as actinomycin D (ActD) and Nutlin-3a, a p53 activator, suggesting that the p53 system is functional in immortalized SAECs (Figure 1F).

Under these conditions, we examined the effect of oncogenic KRAS activation and p53 inactivation on cell motility, invasiveness, and EMT, which are thought to be associated with tumor progression (Figure 2A). p53 expression was downregulated by p53-directed small-interfering double-stranded RNAs (si-p53#1 and si-p53#2) in order to elucidate the detailed pathological role of p53 in the regulation of invasion and motility during lung cancer progression. Invasiveness and motility are enhanced by p53 knockdown, as measured by assays using cell-culture

inserts (8 μm pore) coated with or without Matrigel (Figures 2B and 2C). It has recently been reported that p53 inactivation promotes EMT by derepressing Snail expression and upregulating Twist expression, inducers of EMT (Kim et al., 2011; Kogan-Sakin et al., 2011); therefore, we tested whether p53 inactivation elicits EMT in immortalized SAECs. SAECs were infected with either control viruses or $KRAS^{V12}$ expression viruses, followed by infection with either control viruses or p53-directed short-hairpin double-stranded RNAs (shp53) expression viruses, and expressions of KRAS and p53 in stable transformants were confirmed by immunoblot analysis (Figure 2D). For this experiment, $KRAS^{V12}$ expression was maintained at low level because overexpression of oncogenic KRAS induced cell growth arrest such as oncogene-induced cellular senescence. Even if ectopic KRAS expression is only slightly higher than endogenous expression, activation of downstream MAPK pathways but not AKT pathways in SAECs expressing oncogenic KRAS could be detected, as assayed by immunoblotting (Figure 2D). Under these conditions, p53 knockdown did not induce an EMT-like phenotype (Figure 2E, cf. panel 1 to panel 3), as judged by morphological changes, downregulation of E-cadherin, an epithelial marker and upregulation of mesenchymal markers including N-cadherin and Vimentin (Figure 2F, cf. lane 1 to lane 3). These data suggest that p53 seems not to regulate EMT, at least under our conditions, using immortalized cells of normal lung epithelial cell origin. KRAS gene mutations have often occurred in atypical adenomatous hyperplasia (AAH) and bronchioloalveolar carcinoma (BAC) observed in the early event of lung pathogenesis (Iwakawa et al., 2008; Kitamura and Okudela, 2010); therefore, we assessed the effect of KRAS activation on EMT in SAECs. Interestingly, the expression of $KRAS^{V12}$ in SAECs gives rise to the EMT-like phenotype, as determined by cell morphology (Figure 2E, compare panels 1 and 3 to panels 2 and 4) and expression of EMT markers (Figure 2F, compare lanes 1 and 3 to lanes 2 and 4). More intriguingly, $KRAS^{V12}$ expression did not enhance invasive and motile activities (Figure 2G, compare panels 1 and 2 to panels 3 and 4), as seen in p53-depleted SAECs, suggesting that the EMT-like phenomenon does not appear to link to invasiveness and motility and that alternative p53 pathways contribute to the aggressiveness.

Identification of p53-Regulated Genes Encoding Cell-Surface Proteins Responsible for Cell Invasion and Motility

To elucidate the mechanism by which p53 loss enhances invasive and motile activities in SAECs, we performed comprehensive expression profiling analyses between p53 knockdown and control cells using GeneChip Human Genome U133 plus 2.0 arrays. These experiments showed that 29 genes were upregulated (fold induction, >2) and 28 genes were downregulated (fold reduction, <0.5) in p53-knockdown SAECs (Figures 3A). Among them, nine genes (CLIC4, IL6ST, TMEM87B, TMEM64, FZD2, EMP2, CHRNA1, TSPAN2, and CA9) encoding a cell-surface protein derepressed by p53 knockdown were selected, because membrane-spanning cell-surface proteins have emerged as key regulators in invasion, motility, and metastasis, and, as a future perspective, antibodies and nucleic acid aptamers against such proteins may be utilized as targets for cancer therapy (Deonarain et al., 2009; Dua et al., 2011; Haeuw et al., 2011; Hemler, 2008). Among these nine genes, TSPAN2 was an uncharacterized factor, and the high expression level of TSPAN2 was significantly associated with poor prognosis, although a significant association of high expression of other genes with poor prognosis was not observed in the same samples (Figures 3B and S1; Table S1A). We further assessed which genes are actually derepressed by p53 inactivation. Expression level of TSPAN2 was significantly associated with the p53 mutation status in lung cancer cell lines (Iwakawa et al., 2010), as measured by quantitative real-time PCR (Figure 3C; Table S1B), and TSPAN2 expression in lung cancer cells harboring deletion, null, and missense mutations of p53 was significantly higher than that in cells harboring wild-type p53 (wild-type p53 versus deletion and null p53, $p = 0.0268$; wild-type p53 versus missense p53, $p = 0.00876$; Figure 3C). In addition, TSPAN2 expression in lung cancer cells harboring missense mutations of p53 was moderately, but not significantly, higher than that in cells harboring deletion and null mutations of p53 (deletion and null p53 versus missense p53, $p = 0.095$; Figure 3C).

We also confirmed that TSPAN2 was derepressed by p53 knockdown in SAECs using quantitative real-time PCR (Figure 3D) and immunoblotting with anti-TSPAN2 antibody (Figure 3E). In addition, treatment of cells with Nutlin-3a decreased TSPAN2 expression (Figure S2A), and the decrease was in a p53-dependent manner (Figure S2A). However, p53 knockdown had little or no effect on TSPAN2 expression in MCF7 cells, a human mammary carcinoma cell line (Figure S2B), although TSPAN2 expression in SAECs treated with si-p53 significantly increased compared with that in control cells (Figure S2C), suggesting that p53 regulates the expression level of TSPAN2 with some tissue specificity. In addition, knockdown of mutant p53 in EBC1 cells decreased TSPAN2 expression (Figure S2D), suggesting that mutated p53 has some potential to activate TSPAN2 expression. Furthermore, the high expression level of TSPAN2 was significantly related to p53 mutation in patients with lung ADCs ($p = 0.005$; Figure 3F). Thus, we speculate that the expression level of TSPAN2 in cells is maintained at a low level by the expression of wild-type p53 and focused on TSPAN2 in later analyses.

TSPAN2 Regulates p53-Mediated Cell Invasion and Motility

TSPAN2 is categorized as a four transmembrane-spanning protein belonging to the tetraspanin family, some members of which have been reported to regulate tumor progression (Hemler, 2008; Romanska and Berditchevski, 2011; Wang et al., 2011). To address whether TSPAN2 contributes to invasion and motility by p53 knockdown, TSPAN2 was downregulated in p53-depleted SAECs. In vitro migration and Matrigel invasion assays showed that TSPAN2 knockdown inhibited invasive and motile activities activated by p53 knockdown, suggesting that TSPAN2 is a factor responsible for invasiveness and motility associated with p53 inactivation (Figures 4A–4C). To address whether TSPAN2 is also involved in invasiveness and motility in other established lung cancer cell lines, we used EBC1 cells highly expressing TSPAN2, which expresses a mutant p53. As expected, cell motility and invasion in EBC1 cells were significantly

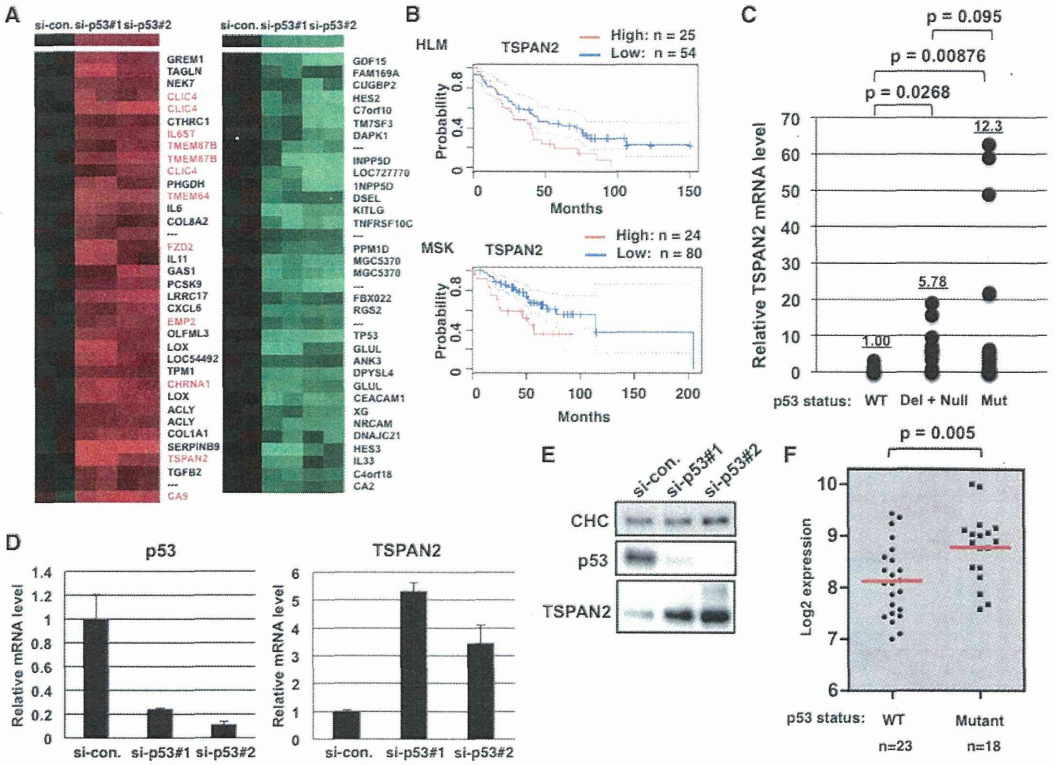

Figure 3. TSPAN2 Is Identified as a Gene Derepressed by p53 Depletion in SAECs, and Its High Expression Is Associated with Poor Prognosis in Patients with Lung ADCs

(A) Genes altered by p53 knockdown in SAECs are indicated. The heatmap shows 29 genes upregulated by p53 knockdown (fold induction, >2) and 28 genes downregulated by p53 knockdown (fold reduction, <0.5).

(B) High expression of TSPAN2 is associated with poor prognosis. Association of expression level of TSPAN2 with the prognosis of NSCLC patients in expression profile studies from KLM and MSK was obtained from the PrognoScan database (Mizuno et al., 2009).

(C) Expression level of TSPAN2 in various human lung cancer cell lines harboring mutant p53 (deletion, null, and missense mutations) is higher than that in cells harboring wild-type p53 (Student's t test, $p < 0.05$). Human lung cancer cell lines used for this assay were listed in Table S1B.

(D and E) p53 knockdown derepressed expression of TSPAN2. Cells were transfected with the indicated siRNAs and total RNA prepared from these cells was subjected to quantitative real-time PCR (D) and immunoblotting (E). Clathrin heavy chain (CHC) is shown as a loading control.

(F) Comparison of expression of TSPAN2 in patient's samples with or without p53 mutations (unpaired t test, $p < 0.05$).

Error bars indicate SD of three independent measurements. See also Figures S1 and S2 and Table S1.

suppressed by TSPAN2 knockdown (Figures 4D–4F). We next tested the effect of TSPAN2 knockdown on H441 cells, a human lung cancer cell line; T98G cells, a human glioblastoma cell line; and DLD-1 cells, a human colorectal cancer cell line, which were all harboring mutant p53. TSPAN2 knockdown decreased cell motility in all cell lines tested, suggesting that TSPAN2 is involved in the aggressiveness of various cancerous cell types including lung, glioblastoma, and colorectal cancer (Figures S3A–S3C). We also examined whether TSPAN2 is contributed to cell motility driven by transforming growth factor (TGF)-β1. Treatment of A549 cells, a human lung cancer cell line, with TGF-β1 increased cell motility, but TSPAN2 knockdown had little effect on cell motility driven by TGF-β1 (Figure S3D). The migratory rate in cells stably expressing small hairpin RNA (shRNA) against TSPAN2 was slower than that of control cells (Figures 4G and 4H); in contrast, forced expression of FLAG-HA-His-tagged TSPAN2 (TSPAN2-FHH) in SAECs (Figure 4I) enhanced migratory activity (Figure 4J) and invasive activity (Figures 4K and 4L); in contrast, FLAG-HA-His-tagged CD82 (CD82-FHH), which is known as a metastasis suppressor belonging to the tetraspanin family (Tsai and Weissman, 2011), did not enhance invasiveness (Figures 4K and 4L). Taken together, TSPAN2 has the ability to promote invasiveness and motility in lung cancers.

TSPAN2 Knockdown Suppresses Tumor Metastasis to Lung

We next assessed whether TSPAN2 affected invasive and metastatic activities into the lungs in vivo. SAECs were infected with lentiviruses for the expression of large T and small T antigens, which inactivate substantial p53 function (Tiemann et al., 1995) compared to p53 knockdown, followed by oncogenic $KRAS^{V12}$ expression to generate $SAEC^{LSK}$ possessing tumorigenicity in immunodeficient NOD-scid, interleukin (IL)-2Rγ-null (NOG) mice (Nakamura and Suemizu, 2008) (Figure S4A). Quantitative

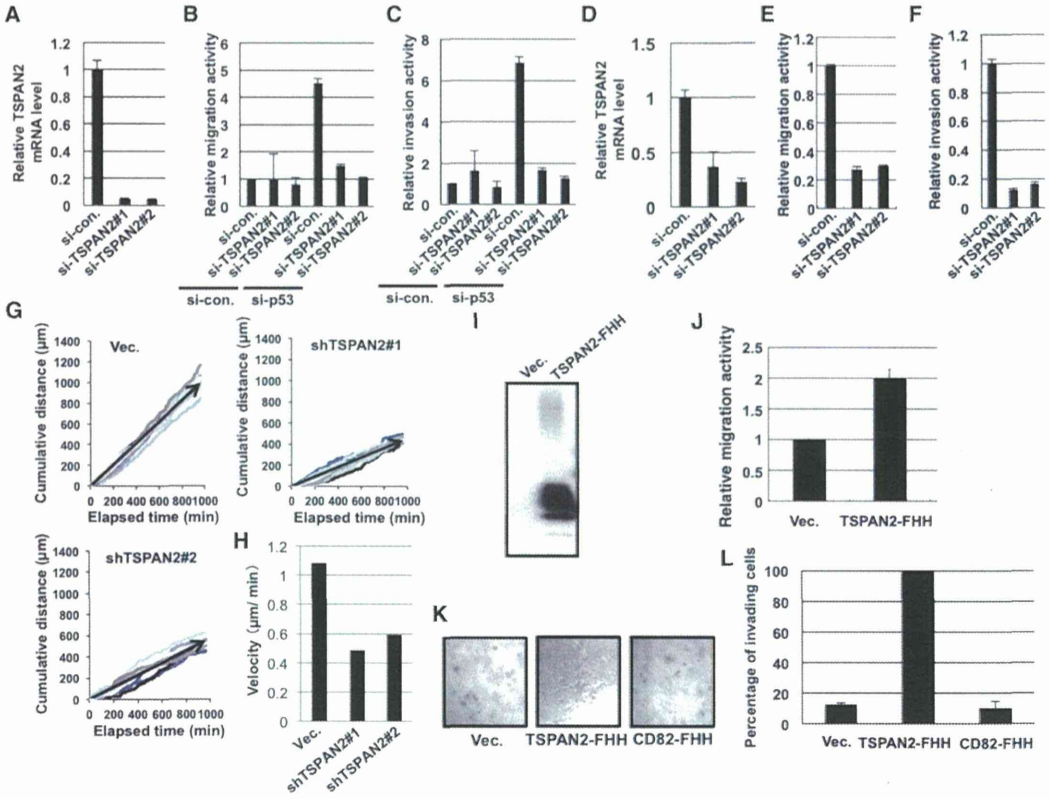

Figure 4. TSPAN2 Regulates p53-Mediated Cell Invasion and Motility

(A) Efficiency of TSPAN2 knockdown in SAEC was determined by quantitative real-time PCR.

(B and C) Inhibition of p53-inactivation-mediated motility (B) and invasiveness (C) in immortalized SAECs by TSPAN2 knockdown.

(D) Efficiency of TSPAN2 knockdown in EBC1 cells was determined by quantitative real-time PCR.

(E and F) Inhibition of motility (E) and invasiveness (F) in EBC1 cells.

(G and H) Attenuation of migratory rate in SAECs by TSPAN2 knockdown. The cell movements for ten cells were analyzed using AxioVision Version 4.8 Cell Tracking software (G). Velocity of the cell movements was calculated by the ratio of cumulated distance to elapsed time (H).

(I) Expression level of TSPAN2 in SAECs infected with lentiviruses with or without TSPAN2-FHH.

(J) Cell motility in SAECs stably expressing TSPAN2-FHH.

(K and L) Invasive activity in SAECs stably expressing TSPAN2-FHH or CD82-FHH using 3D-Matrigel invasion assay. Photograph of invading cells under light microscope (K). Quantification of invading cells (L). Error bars indicate SD of three independent measurements.

See also Figure S3.

real-time PCR experiments revealed that large T and small T antigens as well as p53 knockdown resulted in upregulation of TSPAN2 (Figure S4B), indicating that TSPAN2 expression increases in SAECs expressing large T and small T antigens compared with those expressing wild-type p53. Under these conditions, $SAEC^{LSK}$ stably expressed shRNA against TSPAN2 ($SAEC^{LSK}$-pL-shTSPAN2), the expression level of TSPAN2 was measured using RT-PCR (Figures 5A and S4C), and metastatic activity was assessed in NOG mice. For real-time imaging in vivo, a luciferase gene was introduced into $SAEC^{LSK}$-pL-shTSPAN2, and these cells were inoculated into the tail vein of mice. Under in vitro culture conditions, TSPAN2 knockdown had little or no effect on cell proliferation (Figure S4D) or anchorage-independent growth in soft agar (Figure S4E), whereas TSPAN2 knockdown abrogated cell motility (Figure 5B) and invasive activity (Figure 5C) in vitro, and metastatic activity to lung tissues, as visualized by in vivo imaging using an IVIS system (Figure 5D). Most mice inoculated with TSPAN2-depleted cells were still alive at 48 days postinoculation, although all mice inoculated with $SAEC^{LSK}$ control cells had died by this time point (Figure 5E). Histological analyses using hematoxylin and eosin staining showed that control cells invaded lung organs to a much greater extent and exhibited liver metastases (Figure 5F); in contrast, TSPAN2-depleted cells (#1 and #2) slightly invaded the lungs but had little metastatic activity to other organs (Figures 5G and 5H).

TSPAN2 Knockdown Increased the Production of Reactive Oxygen Species through CD44 to Inhibit Invasive and Motile Activities

What is the mechanism by which TSPAN2 controls invasiveness, motility, and metastasis? To investigate this mechanism, we

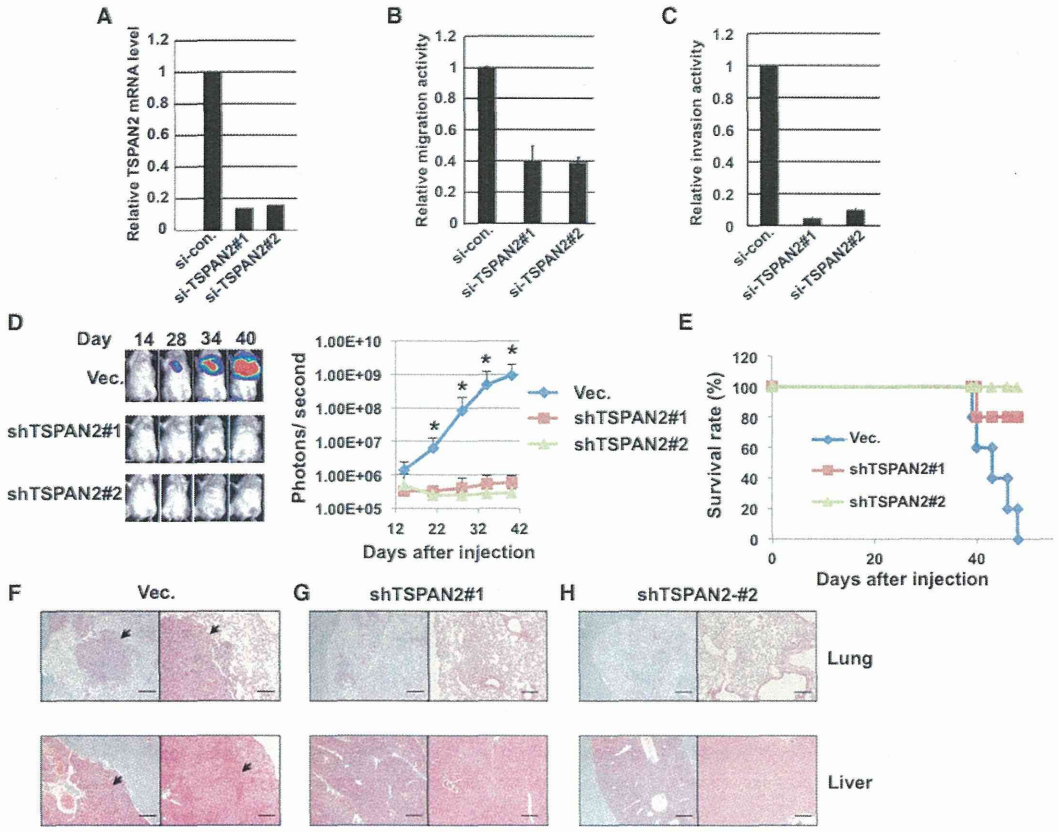

Figure 5. TSPAN2 Knockdown Suppresses Tumor Metastasis to Lung

(A) Efficiency of TSPAN2 knockdown in SAEC^{LSK}. Cells were transfected with the indicated siRNAs, and the expression level of TSPAN2 was determined by quantitative real-time PCR.

(B and C) TSPAN2 knockdown in SAEC^{LSK} decreases cell motility (B) and invasive activity (C).

(D) Suppression of metastatic activity of SAEC^{LSK} by stable expression of shTSPAN2 in vivo. SAEC^{LSK} were infected with lentiviruses encoding luciferase and inoculated intravenously in NOG mice. Time kinetics of lung metastasis in mice was measured using a real-time in vivo imaging system (left). Tumor growth in lungs was quantified using Living Image software (right) ($n = 5$, $^*p < 0.01$ versus vector control).

(E) Survival curve of mice that had been transduced with SAEC^{LSK} with or without the expression of shTSPAN2.

(F–H) Hematoxylin and eosin staining of paraffin sections in metastasized lung and liver tissues in mice inoculated with control cells (F), shTSPAN2#1-expressing cells (G), or shTSPAN2#2-expressing cells (H). Metastasized cancers are indicated with arrows.

Scale bars, 200 μm (right panels) and 500 μm (left panels). Error bars indicate SD of three independent measurements. See also Figure S4.

explored binding partners for TSPAN2. In the immunoprecipitation assay, we used CD82 to compare these binding partners. TSPAN2-FHH or CD82-FHH was stably expressed in cells and sequentially immunoprecipitated with anti-FLAG and anti-HA antibodies. Proteomic databases for proteins belonging to the tetraspanin family predict that several proteins, including CD44, MT1-MMP, ADAM10, and integrins, are candidates as binding partners (Le Naour et al., 2006; André et al., 2006; Xu et al., 2009). Therefore, the eluates from anti-FLAG antibody-immobilized beads were subjected to immunoblotting with anti-CD44, anti-MT1-MMP, anti-ADAM10, and anti-integrin antibodies because these proteins are involved in cell motility and invasion in cancers. Immunoblot analyses showed that TSPAN2-FHH bound to all proteins tested; in contrast, CD82-FHH did not (Figure 6A), suggesting that TSPAN2 contributes to various signaling pathways, consistent with the fact that several tetraspanin proteins function as integrators for various signals, including TGF-β and EGFR pathways (Murayama et al., 2008; Sadej et al., 2010). To identify the key signaling pathway for invasiveness and motility, we first tested the effect of TSPAN2 expression on CD44 shedding because MT1-MMP and ADAM10 are known to cleave CD44, and the cleaved cytoplasmic domain of CD44 enters the cytoplasm to promote invasion (Nakamura et al., 2004; Stamenkovic and Yu, 2009); however, TSPAN2 knockdown had little or no effect on ectodomain cleavage of CD44 (Figure S5A). In addition, forced expression of TSPAN2 had little or no effect on CD44 cleavage (Figure S5B). Next, as shown in recent reports, mutant p53 promoted invasion via integrin trafficking (Muller et al., 2009, 2011). Therefore, we next assessed whether the expression of TSPAN2 influenced the recycling of integrin alpha2beta1, which binds to TSPAN2; however, recycling activity was not affected by TSPAN2